Indian Journal of Advances in Chemical Science

Research Article

Synthesis of Cloisite 30B and Graphene Oxide Doped Poly(Acrylamide-co-2-acrylamido-2-methylpropane sulfonic acid) based pH Responsive Nanocomposite Hydrogel as Effective Adsorbent for Removal of Methylene Blue from Aqueous Media

Hlaing Hlaing Myint[1,2], T. J. Sudha Vani[2], N. Sivagangi Reddy[2,3], K. S. V. Krishna Rao[2]*

[1]Department of Chemistry, University of Mandalay, Mandalay, Myanmar, [2]Polymer Biomaterial Design and Synthesis Lab, Department of Chemistry, Yogi Vemana University, Kadapa, Andhra Pradesh, India, [3]Department of Polymer Science and Engineering, Pusan National University, Busan, Republic of Korea.

ABSTRACT

Removal of dyes through adsorption from wastewater has investigated substantial interest nowadays. Acrylamide (AAm)/2-acrylamido-2-methylpropane sulfonic acid (AMPS)/Cloisite 30B clay (AMPS/Clay) hydrogel for the adsorbtion of methylene blue (MB) dye from aqueous solutions was investigated, and the adsorption efficiency was improved by incorporating graphene oxide (AAm-AMPS/GO) in the adsorbent structure. These hydrogels were prepared by free-radical crosslinking copolymerization of AAm and AMPS at 60°C in the presence of N,N'-methylene bis(acrylamide) as the crosslinker. The resulting hydrogels were characterized by Fourier transform infrared spectroscopy, scanning electron microscopy, and X-ray diffraction. The resulting hybrid networks were used as an adsorbent to study the swelling ratio, and the effectiveness in the removal of MB using the adsorption kinetics, pseudo-first and second orders, Langmuir, and the Freundlich adsorption isotherm models. The adsorption equilibrium capacity reached 11.66 mg/g (94.72%) using the AAm-AMPS, 11.77 mg/g (95.13%) using the AAm-AMPS/Clay, and 11.38 mg/g (93.3%) using the AAm-AMPS/GO at 80 min. The effects of various experimental parameters, such as contact time, solution pH, and adsorbent dosage and initial concentration of dye solution, were investigated.

Key words: Acrylamide-2-acrylamido-2-methylpropane sulfonic acid, Adsorption isotherm, Adsorption kinetics, Hybrid-hydrogel, Methylene blue, Swelling ratio

Graphical Abstract

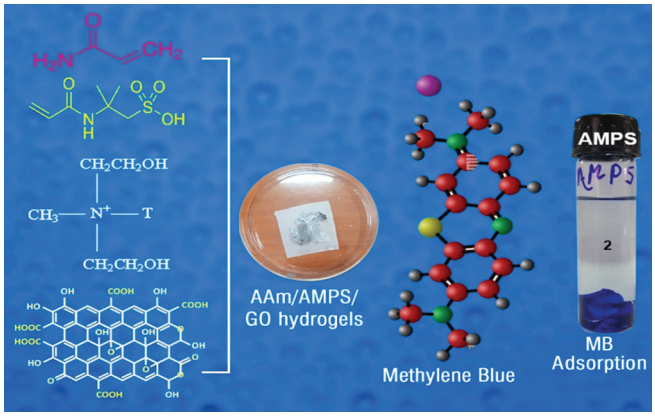

1. INTRODUCTION

In recent years, hydrogels derived from acrylamide (AAm) have received considerable attention for use as specific adsorbents for wastewater treatments. Hydrogels are a kind of cross-linked polymeric network with high water-absorbing and water-retaining capacity. Hydrogels are among the most widely studied materials as an adsorbent for organic dye removal from wastewater owing to their excellent water absorption, high porosity, easy handling, and facile preparation [1-5]. Especially, graphene oxide (GO) has been proposed as a potential replacement for existing polymeric composites for desalination and water purification processes because it can be used as a building block for multi-layered laminated structures. The biodegradable adsorbent hydrogel polymer or polymer composites, such as Cloisite 30B clay-based composites can be used for potential MB adsorption and subsequently reuse the spent hydrogel for consecutive adsorption cycles [6].

Due to the presence of ionizable carboxylic and hydroxyl groups in the polymer network, hydrogels can act as potential adsorbents [7-13]. It remains a major challenge to find cheaper and environmentally friendly technologies for dye removal from textile wastewater. Due to their complex and stable structures, the degradation of dyes in nature is usually very difficult and slow; as a consequence, they accumulate. GO sheets have become a target of numerous studies for dye removal from wastewater. As GO has a two-dimensional structure, GO possesses a

***Corresponding Author**
K. S. V. Krishna Rao,
E-mail: drkrishnaraoyvu@gmail.com

ISSN NO: 2320-0898 (p); 2320-0928 (e)
DOI: 10.22607/IJACS.2026.1402002

Received: 15th March 2026;
Revised: 25th April 2026;
Accepted: 28th April 2026;
Published: 04rd May 2026

greater affinity for dye molecules through π-π stacking interactions [14]. GO has oxygen-rich functional groups such as carboxyl, carbonyl, and hydroxyl groups, which can increase electrostatic interactions with dye cations. Organic dyes put on grave health and environmental hazards to the ecosystem. Hydrogels suffer from a lack of mechanical stability and recovery as compared to synthetic polymers. We employed one method to improve the mechanical stability and separation of the hydrogel in removing methylene blue (MB) dye from aqueous solutions. Organic dyes widely used in textiles, cosmetics, and printing are causing serious pollution to water bodies, giving unsavory after-effects.

Cationic dyes,such as MB, are chemicals that cause serious environmental pollution and pose threats to human health, and are often carcinogenic and/or mutagenic in nature. Due to the toxic effects of dyes, their removal from wastewater has become an important aspect in the field of water remediation. Therefore, the removal of dyes from aqueous solutions is always widely focused. Many methods have been used to remove dyes, such as chemical precipitation, membrane, coagulation and flocculation, electrochemical treatment, ion-exchange, and adsorption. Among these methods, adsorption shows advantages over others for its high efficiency, good selectivity, low cost, and easy regeneration.

The aim of the present research is to develop Cloisite 30B and GO-doped poly(acrylamide-co-2-acrylamido-2-methylpropane sulfonic acid) based pH-responsive nanocomposite hydrogels. Furthermore, to explore the various kinetic models, swelling properties of hydrogels were performed at different temperatures and the adsorption of cationic dye, i.e., MB, on different operating conditions, including pH, contact time, and initial concentration, the temperature of linear forms of equilibrium isotherms.

2. EXPERIMENTAL

2.1. Materials

Analytical reagent grade samples of 2-acrylamido-2-methylpropane sulfonic acid (AMPS) and Cloisite 30B clay were purchased from Aldrich Chemicals Co., Ltd., USA. AAm, Graphite powder, and MB were purchased from Merck Specialties Pvt. Ltd., Mumbai, India. All chemicals were used without further purification, and double-distilled (DD) water was used throughout the experiments.

2.2. Preparation of GO

GO was prepared using the modified Hummers' method [15]. 0.5 g of graphite was added to a 250 mL beaker. Then, 0.5 g of sodium nitrate and 23 mL of concentrated sulfuric acid were added with continuous stirring on a hotplate magnetic stirrer, and the mixture was placed in an ice-water bath for 4 h. Then, 3 g of potassium permanganate was slowly added to this mixture. After that, the mixture was continuously stirred for 1 h in the ice-water bath and was heated at 35°C for 1 h. To this mixture, 46 mL of distilled water was added, and the mixture was stirred well and heated up to 98°C for 2 h. The reaction was ended by adding 100 mL of distilled water and 10 mL of H_2O_2 aqueous solution, to yield a yellow slurry. Finally, the mixture was filtered with filter paper and washed with 5% hydrochloric acid (HCl) and distilled water using a centrifuge to remove acid and metal ions. Then, the GO and the strong acid filtrate were obtained. The GO was dried in an oven at 60°C for 10 h.

2.3. Preparation of Hybrid Hydrogels

Hydrogels of AAm and AMPS were synthesized by employing free radical polymerization using N,N-methylene bis acrylamide (MBA) as a cross-linker and ammonium persulfate as a free radical initiator. In detail, hydrogels based on AMPS were prepared by first mixing 1 g of AAm and 1.4561 g of AMPS to form the AAm-AMPS hydrogel. Another set of hydrogels was also synthesized by mixing 0.2456 g Cloisite 30 B (AAm-AMPS/Clay) or 0.0245 g GO (AAm-AMPS/GO) in 5 mL water. The hydrogels (AAm-AMPS, AAm/AMPS/Clay, and AAm-AMPS/GO) were washed and soaked overnight in distilled water by changing the DD water to remove any unreacted monomers. The resulting composite hydrogels were removed from the reaction vessel and cut up into small pieces. These gels were dried first at room temperature and finally in a hot air oven at 45°C up to constant weight.

2.4. Swelling Measurements

The equilibrium swelling ratio (ESR) of hydrogel (AAm-AMPS, AAm-AMPS/Clay, and AAm-AMPS/GO) was investigated by immersing them in 100 mL distilled water at different temperatures (18, 28, and 38°C). The ESR was calculated using Equation (1),

$$Equilibrium\ Swelling\ Ratio\ (ESR) = \frac{W_f}{W_i} \times 100\ \% \quad (1)$$

where W_i is the initial mass of dried gel, and W_f is the constant mass of swollen hydrogel at equilibrium.

2.5. Adsorption Experiments

Adsorption of MB on (AAm-AMPS), AAm-AMPS/Clay, and AAm-AMPS/GO was carried out using a batch experiment method on a magnetic shaker. The effect of contact time, solution pH, and adsorbent dosage, and initial concentration of MB dye were investigated.

2.5.1. Dye adsorption studies

MB adsorption experiments started with the preparation of a MB stock solution of 100 mg/L to prepare MB solutions of various desired concentrations. A linear calibration curve of MB was analyzed from absorbance measurements of 2, 4, 6, 8, and 10 mg/L MB solutions. These experiments were carried out by adding a fixed amount of adsorbent, 0.02 g of AAm-AMPS, into each conical flask and mixing with 25 mL of (10 mg/L ppm) MB dye. These container bottles containing the mixture were placed in a magnetic stirrer at room temperature. The absorbance was measured at the MB maximum absorption wavelength at λ_{max} = 660 nm using an ultraviolet-visible spectrometer.

2.6. Batch Mode Experimental Protocol

The concentration of MB before and after adsorption was measured from absorption values, further converted to concentration using a linear calibration curve. The removal ratio (R%) and the adsorption capacity (Q_e) for MB were calculated using Equations (2) and (3).

$$Removal\ \% = \frac{C_0 - C_e}{C_0} \times 100\ \% \quad (2)$$

$$Q_e = C_0 - C_t \times \frac{V}{m} \quad (3)$$

where C_0 (mg/L), C_t (mg/L), and C_e (mg/L) are MB concentrations at initial time, time t, and equilibrium concentration, respectively, V (L) is the volume of MB dye solution used, and m (g) is the weight of dried adsorbent. All the experiments were carried out in triplicate, and results were represented for the average of the three readings and calculated using Equations (2) and (3).

The effect of adsorbent dosage on MB adsorption was carried out to set the adsorbent dose for the remaining of the adsorption experiments. Different adsorbent doses were added to 25 mL of the MB solution of concentration 10 mg/L at room temperature, and at a solution pH of 6.6, a magnetic stir at a constant speed of 100 rpm was used to

maintain quality control of measurements. The final MB concentration was determined after 80 min of contact time. The initial pH of this solution was adjusted using a pH meter with 0.1 N HCl and 0.1 N sodium hydroxide in the range of pH 2, 4, 6, and 8. The final MB concentration was determined after 130 min of contact time.

3. RESULTS AND DISCUSSION

3.1. Fourier Transform Infrared Spectroscopy (FTIR) Analysis

FTIR measurements were carried out on the nanohydrogel copolymer (AAm/AMPS). FTIR spectra were obtained using an infrared spectrometer (Shimadzu, Japan) in the 4000–500 cm^{-1} region at room temperature [Figure 1]. Furthermore, we characterized hydrogel and nanocomposite samples before and after MB adsorption by FTIR.

High adsorption efficiency of MB was correlated to the new structural characteristics and the functional groups of the polymer composite. The peak at 2934 cm^{-1} is related to the stretching (C-H) bond from CH_2 groups of alkyl chains. A peak present at 1647 cm^{-1} is attributed to the stretching vibration of C=O (amide I band) from the amide group. The band at 1036 cm^{-1} in the spectrum of poly(AMPS-co-AAm) is assigned to the symmetric stretching of the S=O group [16].

FTIR confirmed the changes of the functional group after the MB blue dye adsorption process, indicating a uniform shape for the carboxylate hydrogels compared to the non-functionalized hydrogels based on AAm units on Clay or GO. Specifically, the adsorption equilibrium reached 20 mg/g in 80 min after the surface modification of the polymer composites.

Due to the abundant carboxyl and amino groups in AAm-AMPS added to the composite structure, a high adsorption capacity for MB dyes removal has been provided. In particular, the adsorption equilibrium of MB for composite hydrogels was higher than that of unmodified AAm-AMPS (pure hydrogel).

3.2. SEM Analysis

Scanning electron microscopy (SEM) was used to study the morphology of the AAm-AMPS, AAm-AMPS/Clay, and AAm-AMPS/GO [Figure 2]. The morphology of the prepared composite hydrogels was investigated by SEM. After the composite formation of Clay or GO, the surface of the AAm-AMPS/Clay and AAm-AMPS/GO became rougher compared to the incomposite hydrogel AAm-AMPS in Figures 3-5. The SEM images (AAm-AMPS) show dense, irregular lamellated granules with a typical polymeric network [Figure 2] [17]. The SEM image of AAm-AMPS/GO indicated that the basic mud cake showed distinct, stacked, crumpled edges and rough-shaped particles. Chemical modification of the composite structure is important to note that the removal efficiency of the adsorbed MB dyes has been increased [14].

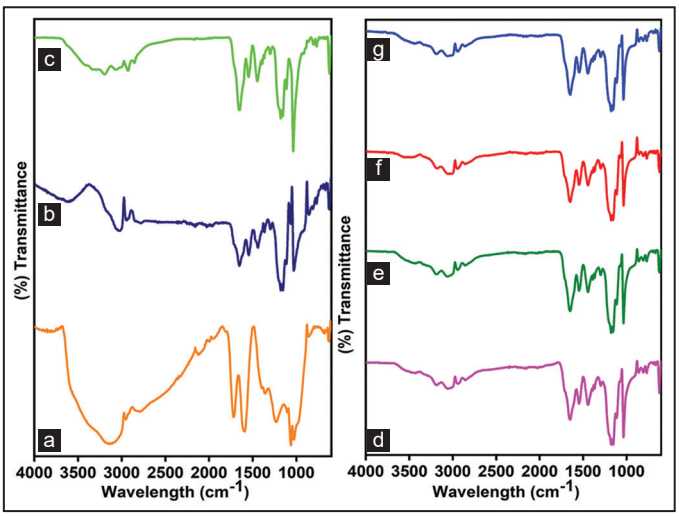

Figure 1: Before and after adsorption of methylene blue into Acrylamide (AAm)-2-acrylamido-2-methylpropane sulfonic acid (AMPS) (a) Pure graphene oxide (GO), (b) AAm-AMPS/Clay before, (c) AAm-AMPS/Clay After, (d) AAm-AMPS/GO before, (e) AAm-AMPS/GO after, (f) AAm-AMPS/Pure hydrogel before, and (g) AAm-AMPS/Pure hydrogel after.

3.3. XRD Analysis

XRD patterns [Figure 6] of all the Am-AMPS-based hydrogels, obtained the peaks at 2θ = 22.3, 27.1, 31.3, and 36.6, were consistent with previous research [18]. In particular, the strong peak at 2θ = 24.3 is a significant marker of the NH group of poly AAm-AMPS hydrogel. This is also a characteristic peak of poly(AMPS) and poly(AAm) due to the decline of crystallinity of poly(AMPS) into copolymer (AAm-AMPS) nanohydrogels. In other words, the increase of poly(AAm) into the hydrogel matrix decreased the crystallinity of copolymer (AAm-AMPS) nanohydrogels [19].

3.4. Swelling Studies of AAm-AMPS-based Hydrogels

Synthesized hydrogels have significant properties, such as mechanical strength, biocompatibility, biodegradability, swelling ability, and stimuli sensitivity. Among these properties, the water absorption capacity or swelling ability of the hydrogel has an important effect on the adsorption behavior for the removal of MB from aqueous solutions.

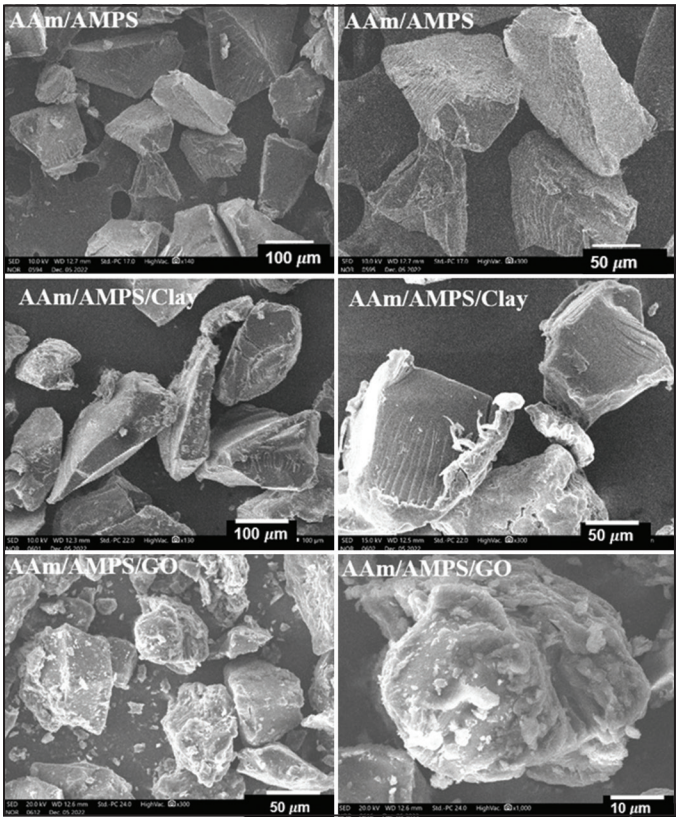

Figure 2: Scanning electron microscopy micrograph of acrylamide-2-acrylamido-2-methylpropane sulfonic acid (AAm-AMPS), AAm-AMPS/Clay, and AAm-AMPS/Graphene oxide hydrogels at dried conditions.

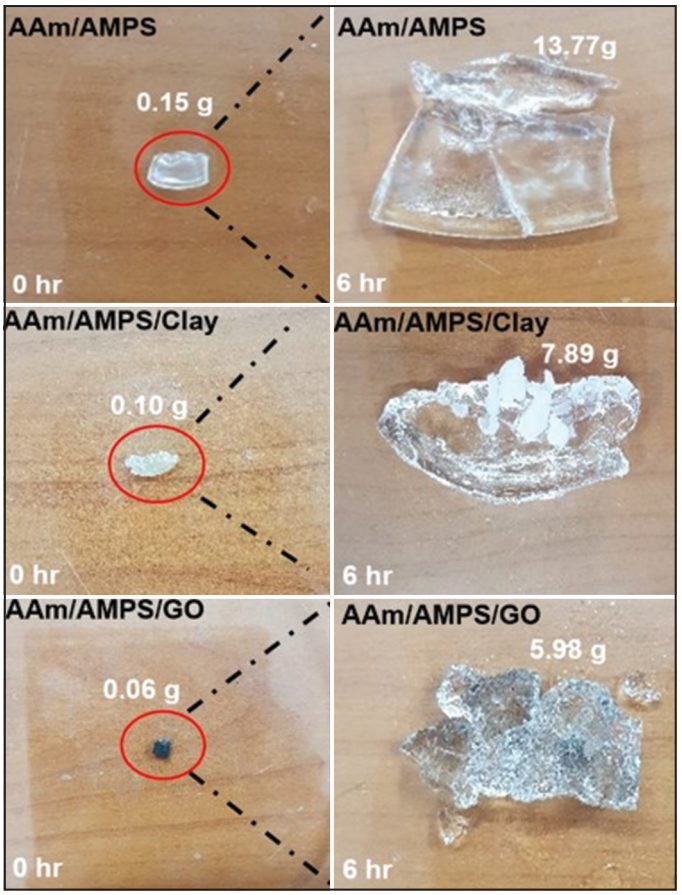

Figure 3: Before and after equilibrium swelling test of hydrogels in water for 6 h at 28°C.

The freshly prepared dried hydrogels and the swollen hydrogel are depicted in Figure 3. In an aqueous system, the temperature sensitivity of a hydrogel is closely related to the polymer-water interactions, hydrogen bonding, and hydrophobic interactions. For AAm-AMPS hydrogels, the swelling behavior was investigated at different temperatures, 18, 28, and 38℃, as shown in Figure 4.

To keep the temperature at 18°C, the hydrogel swelling process was executed in a cooling bath under the control of a thermometer. Hydrogels perform the lowest swelling ability at the lowest temperature, at 18°C, due to the increase in water viscosity, in accordance with the stronger hydrogen bonding, which reduces the movement of water molecules. In contrast, at 28°C, the swelling ratio of the hydrogel composite was higher due to the lower viscosity of water at those temperatures. Subsequently, the water molecules can easily be attracted to the 3D polymeric network of the hydrogel composite, resulting in the increased water absorption capacity of the hydrogel. It was found that the hydrogel/GO nanocomposites exhibited improved swelling capacity compared with the other pure hydrogel and hydrogel/clay. In these hydrolyzed hydrogels/GO, the carboxylate groups in the network are appreciably increased, and higher swelling capacity is achieved. A high swelling capacity can increase the available surface area for MB adsorption to aid improved adsorption capacity and removal efficiency.

At lower temperatures, water molecules in the vicinity of hydrophobic polymer chains are highly hydrogen-bonded, because these hydrogen-bonding interactions decrease the free energy of mixing considerably. Therefore, the polymer swells a little in water at low temperatures.

Whereas the swelling ratios of the hydrogels decreased with increasing temperature of the medium. Because hydrogen bonds weaken between

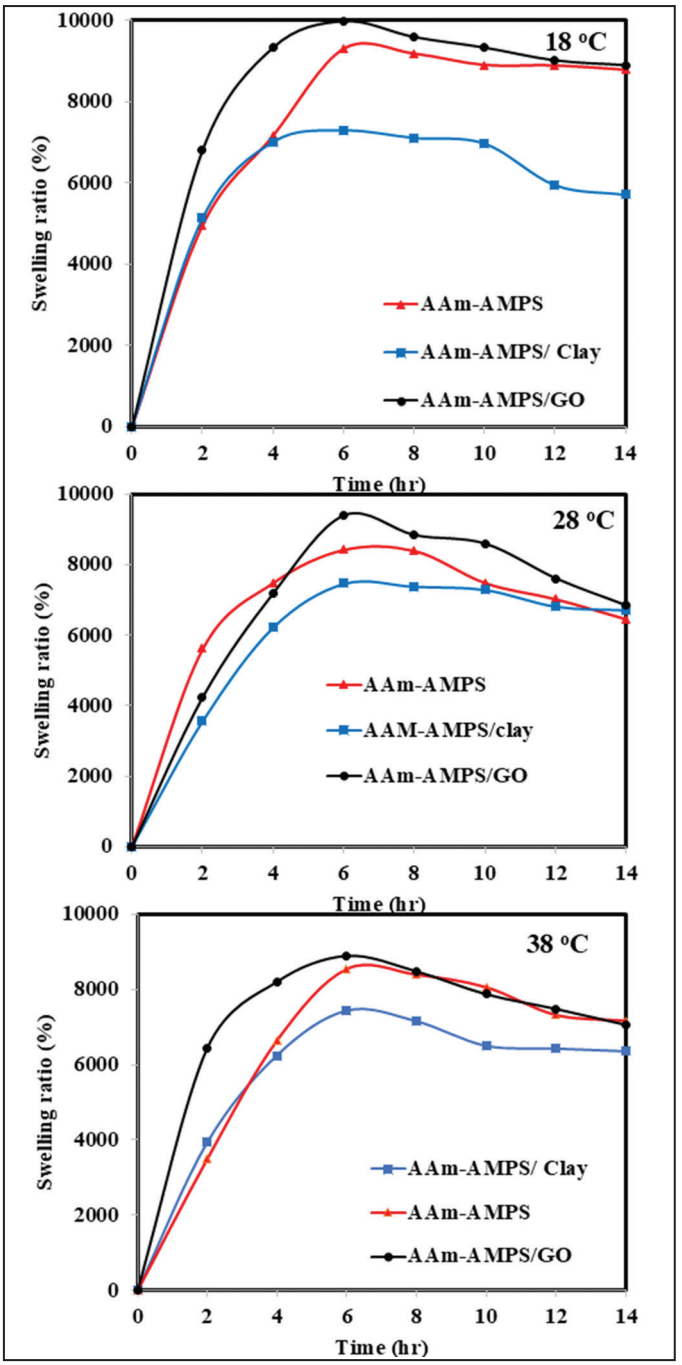

Figure 4: The swelling ratio of Acrylamide/2-acrylamido-2-methylpropane sulfonic acid based hydrogels as a function of time at 18°C, 28°C, and 38°C.

water and hydrophobic surfaces, whereas the hydrophobic interaction increases at higher temperatures. As a result, on heating a polymer gel, a transition from swollen to shrinking state occurs [20]. However, further increase in the swelling time results in the deswelling of the gels until they reach a limiting swelling ratio after about 6 hr at different temperatures.

The swelling ratio data of AAm-AMPS/GO exhibited higher swelling activities at three different temperatures. This is because GO provides enriched oxygenated functional groups, such as -COOH, -C=O, -OH, and -C-O-C- that really attract the water molecules (hydrophilic), which can facilitate interaction between AMPS and AAm within the composite to increase the absorption capacity of the hydrogel [21].

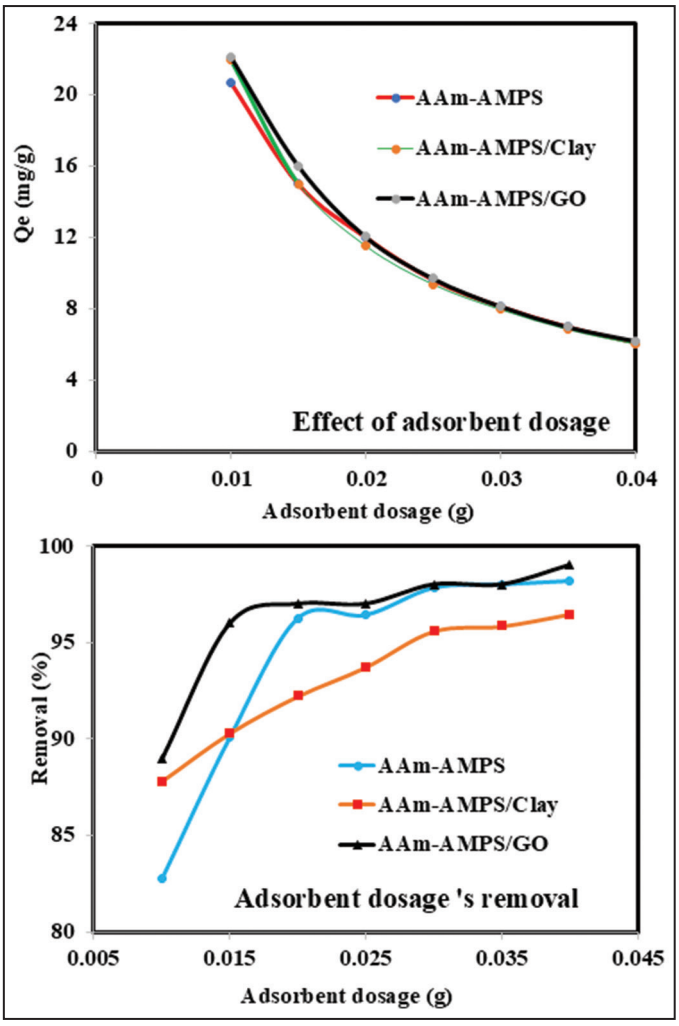

Figure 5: Effect of dosage of adsorbent hydrogels based on Acrylamide-/2-acrylamido-2-methylpropane sulfonic acid, clay, and graphene oxide, and their removal ratio (%).

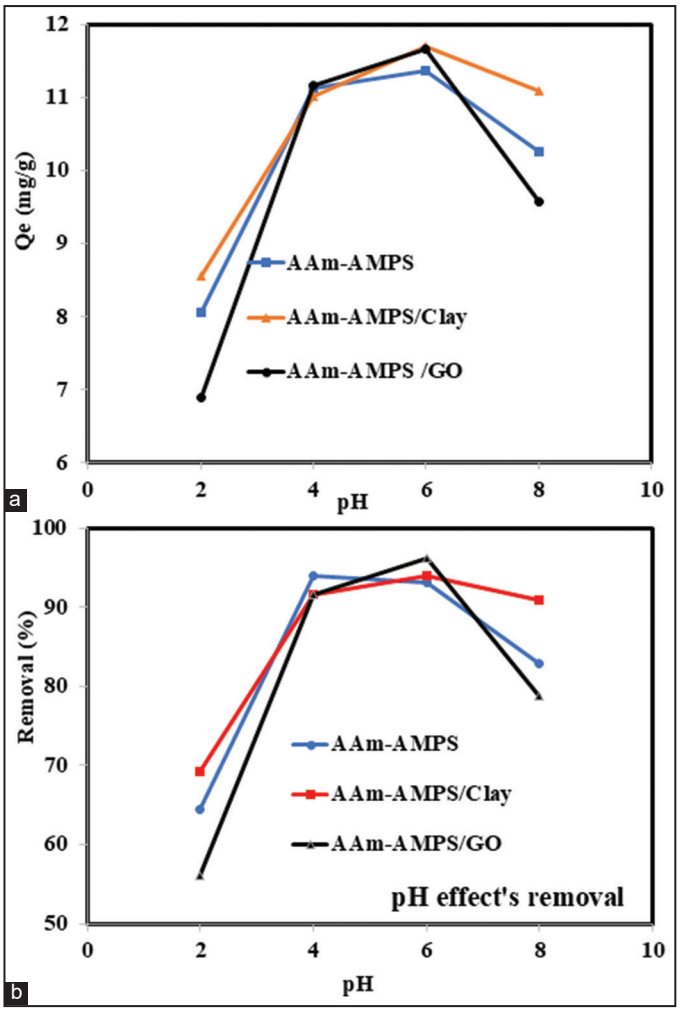

Figure 7: Effect of (a) pH equilibrium adsorption of hydrogels based on acrylamide-2-acrylamido-2-methylpropane sulfonic acid, clay, and graphene oxide, and (b) their removal ratio (%).

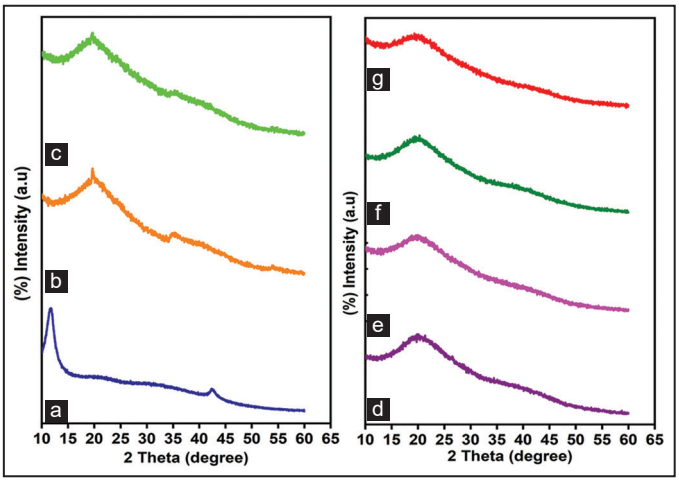

Figure 6: X-ray diffraction analysis of (a) graphene oxide (GO), (b) Acrylamide/2-acrylamido-2-methylpropane sulfonic acid (AAm/AMPS)/Clay before methylene blue (MB) adsorption (c) AAm/AMPS/Clay after MB adsorption, (d) AAm/AMPS/GO before MB adsorption (e) AAm/AMPS/GO after MB adsorption, (f) AAm/AMPS/pure hydrogel before MB adsorption and (g) AAm/AMPS/pure hydrogel after MB adsorption.

3.5. MB Dye Adsorption Studies

3.5.1. Effect of the dosage of the adsorbent

The dosage of adsorbent is one of the important parameters for the adsorption behavior of (AAm-AMPS, AAm-AMPS/Clay, and AAm-AMPS/GO) in the removal of dyes from their aqueous solutions. MB adsorption capacity, i.e., Q_e, decreased with increasing adsorbent dose as shown in Figure 5, whereas the removal percentage remained nearly constant for MB with an increase in the adsorbent dosage from 0.01 to 0.04 g, approximately above 95%. By increasing the adsorbent dose, the adsorption efficiency for all hydrogel and nanocomposite hydrogel types is increased. This can be explained by an increased contact surface of the adsorbents, which facilitates the adsorption process at a higher concentration and adsorptive sites for adsorption. The dye removal increases with an increase in adsorbent dose until a certain limit (35 mg), and then, the rate of increase slows down gradually [22]. Moreover, at higher dosages of adsorbent, adsorption will reach equilibrium quickly because of osmotic pressure, and irrespective of unused active sites. Whereas lower dosages of adsorbent may be readily collapsed, resulting in poor adsorption removal capacity. Therefore, after comprehensive experimentation, a median dose of 0.02 g was selected for the continuation of adsorption experiments [23].

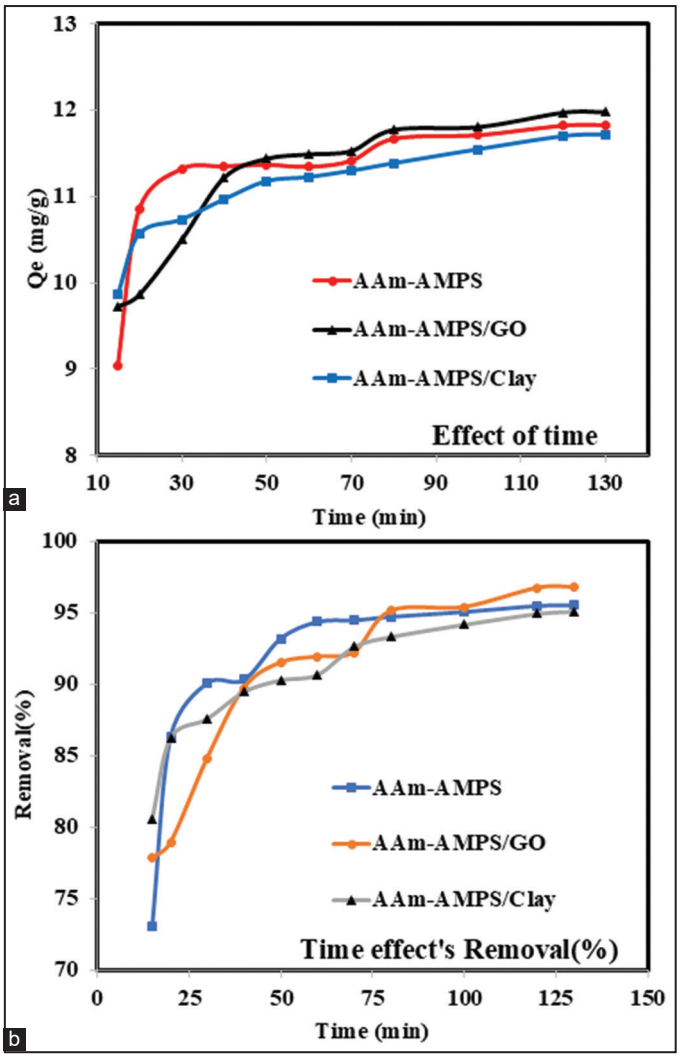

Figure 8: Effect of (a) time effect equilibrium adsorption of hydrogels based on acrylamide-2-acrylamido-2-methylpropane sulfonic acid, clay, and graphene oxide, and (b) their removal ratio (%).

3.5.2. Effect of pH

The effect of the pH of the MB dye solution on the adsorption capacity was investigated. The pH of the MB dye solution on the adsorption capacity was investigated in the MB solution of concentration 10 mg/L in Figures 7a and b.

The low pH value of the dye solution did not show a significant effect on MB adsorption by hydrogels, which was measured at pH = 2 with below 70 % removal percentage. Polymer composite that played AAm-AMPS/GO (-COOH, NH_2, and OH) showed similar behavior for higher removal of cationic MB dye from aqueous solution at pH = 6 with acidic conditions. Thus, it may be because, at alkaline conditions, the ionization of carboxylic functional groups present on the GO surface occurs, and the electrostatic attraction force is increased between the MB and the adsorbent. At pH 8, MB removal efficiencies of AAm-AMPS, AAm-AMPS/Clay, and AAm-AMPS/GO declined to 83, 91, and 79%, respectively, as in Figure 7a and b.

The little high removal adsorption efficiency of MB dyes was correlated to the new structural characteristics of GO and the functional groups of the polymer composite (AAm-AMPS/GO) compared with pure polymer hydrogel (AAm-AMPS) [24].

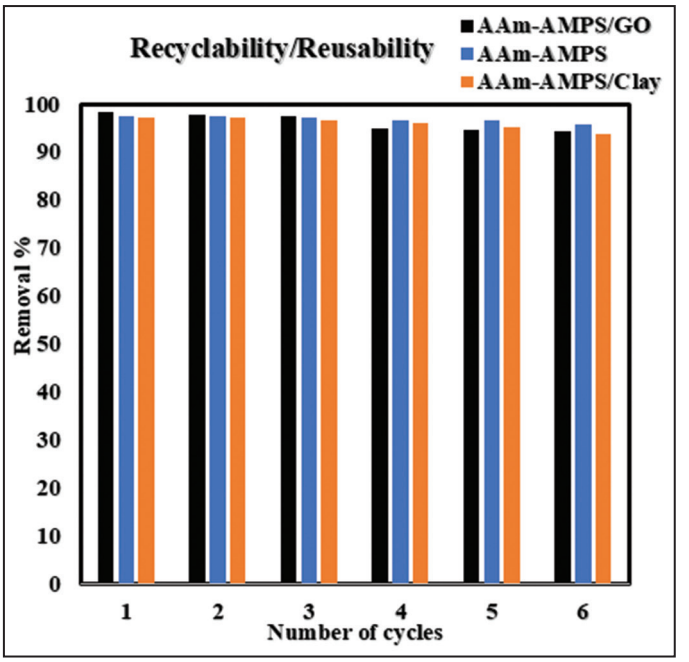

Figure 9: Reusability results of acrylamide-2-acrylamido-2-methylpropane sulfonic acid (AAm-AMPS), AAm-AMPS/Clay, and AAm-AMPS/graphene oxide hydrogel for methylene blue adsorption capacity.

The lower removal ratio can be attributed to the pH approaching the pK of the sulfonate group (pK~1.0) [25] that is responsible for the adsorption of MB via anionic interaction between the adsorbent and cationic dye molecules. In a strongly acidic solution, a competition for adsorption of dye moieties versus H^+ ions exists in addition to the H-bonding and charge-charge repulsion interactions between sulfonate groups from hydrogel and NH of MB with water. The veiling impact of the first positive charges over hydrogels (AAm-AMPS) has diminished. Because of the alkaline medium and empowers the negative effects from the hydrogels to be pulled into the positively charged MB molecules [26].

3.6. Adsorption Kinetics

3.6.1. Effect of contact time

Adsorption kinetics is the most important parameter, and information about the adsorption rate and the adsorption mechanism. exchange, hydrogen bonds, hydrophobic attractions, penetration, diffusion, and adhesion of dye (ion, atom, or molecules) from the solution of the outer surface to internal adsorption into the adsorbent surface of substance site due to the presence of the polymer backbone through chemical bonding, electrostatic interactions, ion, and so on [27]. The effect of time variation on the adsorption capacity of AAm-AMPS, AAm/AAMPS/Clay, or GO for the removal of MB has been investigated in the range of 80 min, as illustrated in Figure 8a and b.

A rapid increase in the adsorption capacity for AAm-AMPS, AAm-AMPS/Clay, and AAm-AMPS/GO is noted during the first 30 min, and afterward, a very slow increase in the MB uptake is observed up to 130 min. The equilibrium adsorption capacity (11.67 mg/g for AAm-AMPS, 11.38 mg/g for AAm-AMPS/Clay, and 11.77 mg/g for AAm-AMPS/GO) is determined at 80 min [28]. Maximum adsorption equilibrium and higher removal percentage of capacity of Aam-AMPS hydrogel is reached 11.77 mg/g (95%) at 80 min, which became constant is shown in Figure 9.

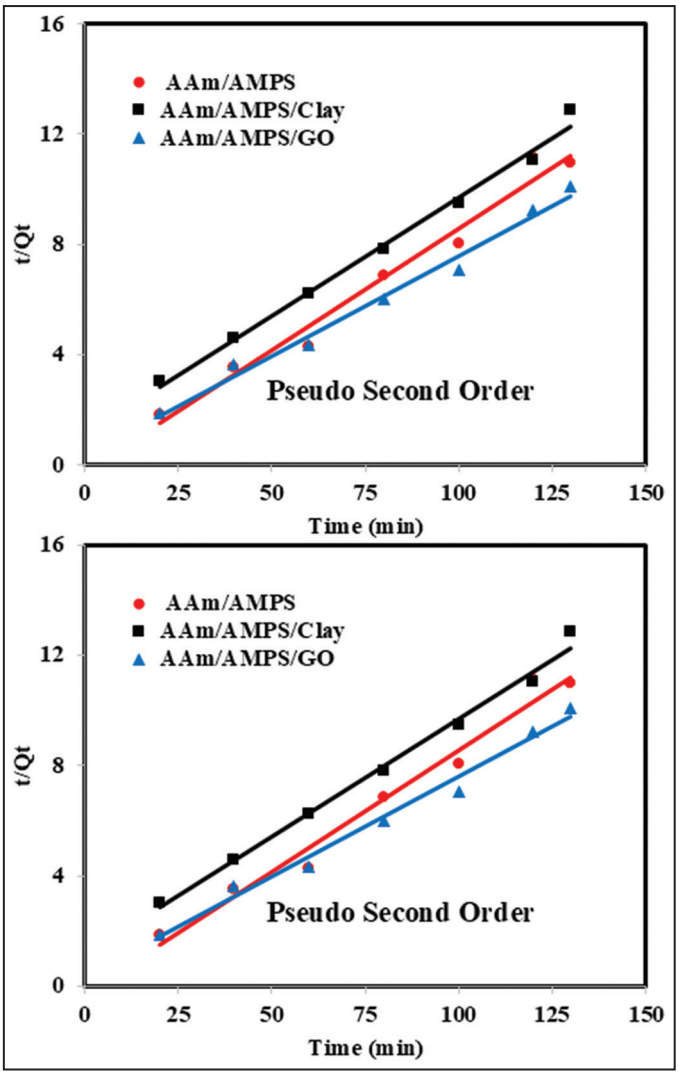

Figure 10: Fitting curves of pseudo-first order and pseudo-second order for adsorption of hydrogels based on acrylamide-2-acrylamido-2-methylpropane sulfonic acid (AAm-AMPS), AAm-AMPS/Clay, and AAm-AMPS/Graphene oxide.

To evaluate adsorption kinetics mechanisms and potential rate-controlling steps, the experimental data were fitted to pseudo-first order (Equation 4) and pseudo-second order (Equation 5).

$$Log\left(C_e - Q_t\right) = Log\, Ce - \frac{K_1}{2.303}t \quad (4)$$

$$\frac{t}{Q_t} = \frac{1}{K_2 Q_e^2} + \frac{t}{Q_e} \quad (5)$$

Where Q_e (mg/g) and Q_t (mg/g) are the adsorption capacity at equilibrium time and time t (min), respectively. k_1 (/min), pseudo first order rate constant, k_2 (g (mg/min)), pseudo second order rate constant. Based on the correlation coefficient (R^2) value, the best fit and most possible adsorption kinetics model for the adsorption is investigated in Figures 10 and 11. Plots are shown in figure, and constants obtained from the plots are summarized in Table 1.

In the case of the pseudo-second order rate model, we found that, at AAm-AMPS/Clay, the regression factor value R^2 is closer to 1 than at the other adsorbent hydrogels (AAm-AMPS and AAm-AMPS/GO). So we can notice that for AAm-AMPS/Clay, second-order kinetics is taking place, which indicates the adsorption method is perhaps a chemical process [29].

According to all the concluding data of kinetic models, A higher correlation coefficient (R^2) value and nearly equal MB adsorption first and second order kinetic constants (K_1) and (K_2) [30].

3.7. Adsorption Isotherm

3.7.1. Effect of concentration

An adsorption isotherm represents the distribution of adsorbate between the adsorbent and solution at equilibrium. The equations used for Langmuir (Equation 6). An important characteristic of the Langmuir isotherm model can be expressed by the separation factor or equilibrium factor (R_L) (Equation 7). R_L = 1 Freundlich (Equation 8) isotherms are as follows:

$$\frac{1}{Q_e} = \frac{1}{Q_{max} K_L}\frac{1}{C_e} + \frac{1}{Q_{max}} \quad (6)$$

$$R_L = \frac{1}{1 + K_L C_e} \quad (7)$$

$$ln\, Q_e = ln\, K_f + \frac{1}{n} ln\, Ce \quad (8)$$

Langmuir and Freundlich are used to describe the adsorption mechanism more deeply based on the concentration of MB in the solution, which was determined after designated time intervals [Figure 12]. The values of Q_{max} and K_L were calculated from the slope and intercept of the linear curve $1/Q_e$ versus $1/C_e$ as presented in [Figure 13] and their data in Table 2.

The Langmuir model uses a monolayer of adsorbate on the surface of the adsorbent, and it assumes that adsorption occurs on a homogeneous surface, without interactions between the adsorbed dye molecules [31].

The R_L values are 0.44, 0.86, and 0.65, confirming the favorability of the adsorption process.

The main assumption of the Langmuir model states that the adsorption process occurs at certain homogeneously identical binding centers on the adsorbent surface. The sorption of the adsorbate occurs at this center. Once the dye occupies the binding site, no further adsorption can occur at this site, and dye molecules cannot interact with each other.

This research also observed a linear curve, ln Q_e versus ln C_e, as presented in Figure 13, that the Freundlich model was best suited for MB adsorption to the hydrogel-based (AAm/AMPS). The values of correlation coefficients of AAm/AMPS/Clay/GO showed a high linearity of 0.95, 0.91, and 0.92, confirming the Freundlich isotherm for adsorption processes.

According to Figure 13 and the fitting parameters presented in Table 2, the data showed that the correlation coefficient value in the Langmuir model (R^2) values which, are higher than that of the correlation coefficient values in the Freundlich model (R^2) and the maximum adsorption capacity of the adsorbent (Q_{max} mg/g). In addition, Junlapong *et al*., 2020, have reported that the values of (*n* values) Freundlich Isotherm $n = (1 < n < 10)$, which suggested that the interaction mechanism was favorable to the adsorption between MB dye molecules and hydrogel surfaces [32]. The high correlation coefficient (R^2) values demonstrate that the adsorption of the MB onto hydrogel (AAm-AMPS) fully obeyed both the Langmuir and the Freundlich isotherms.

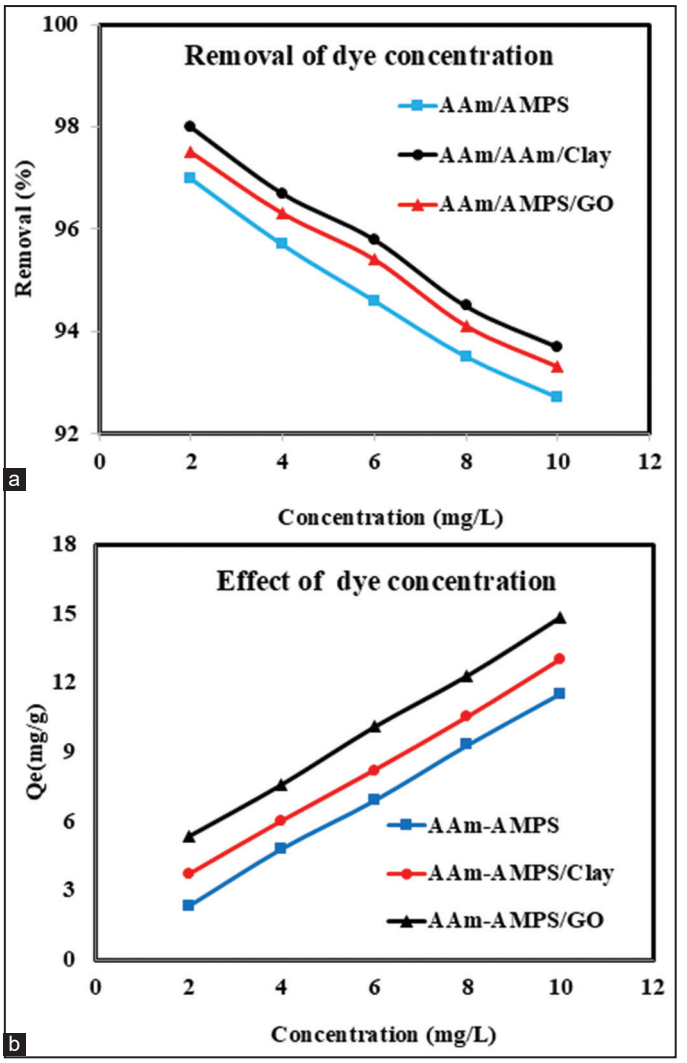

Figure 11: Effect of (a) concentration of dye on equilibrium adsorption of hydrogels based on acrylamide-2-acrylamido-2-methylpropane sulfonic acid, clay, and graphene oxide, and (b) their removal %.

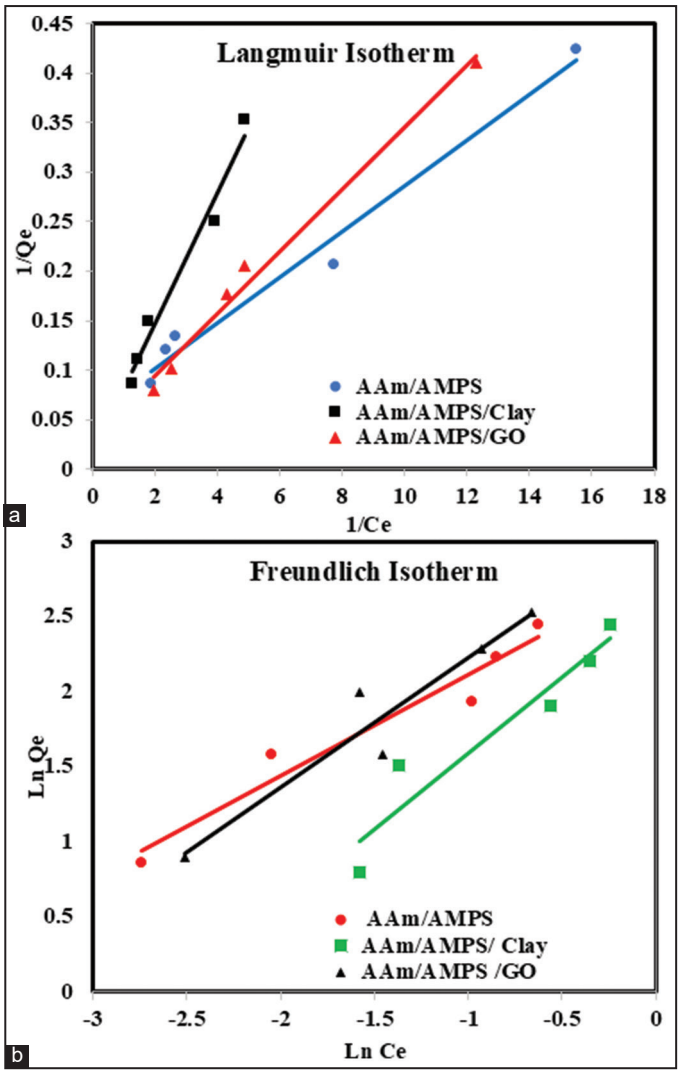

Figure 12: (a and b) Fitting curves of the Langmuir isotherm model and the Freundlich isotherm model for adsorption of hydrogels based on acrylamide-2-acrylamido-2-methylpropane sulfonic acid (AAm-AMPS), AAm-AMPS/Clay, and AAm-AMPS/Graphene oxide.

3.8. Recyclability/Reusability of Cross-Linked based on AAm-AMPS/clay/GO

The capability to recycle and reuse an adsorbent is an essentially important process from the application point of view, and for the economic value of the adsorbent [33-40].

The reusability of the cross-linked AAm-AMPS/clay/GO copolymer hydrogel adsorbent was investigated over five repeat (six total) cycles of the adsorption process, as shown in [Figure 14].

In the 6th repeat cycle, the adsorption capacity was 20 mg/g with a >90% removal efficiency, which supports the reusability of the hybrid hydrogel. A decrease in adsorption capacity in reuse is attributed to a partial, irreversible occupation of hydrogel adsorptive sites by MB dye molecules and a minimal mass loss of the hydrogel during the adsorption and washing cyclic processing. Comparison of our present work with literature is given in Table 3. Therefore, our low-cost, eco-friendly hybrid hydrogel is a promising adsorbent that can be readily recycled and reused several times with high adsorption capacity.

Table 1: Pseudo first order and pseudo second order parameters for MB adsorption on AAm-AMPS, AAm-AMPS/Clay, and AAm-AMPS/GO.

Sample	Q_e (mg/g)	Pseudo-first order		Pseudo-second order	
		K_1 (min^{-1})	R^2	K_2 (min^{-1})	R^2
AAm-AMPS	11.39	0.011515	0.9125	0.0341	0.978
AAm-AMPS/Clay	11.70	0.019345	0.9713	0.0064	0.992
AAm-AMPS/GO	13.79	0.010594	0.9771	0.0153	0.986

MB: Methylene blue, AAm: Acrylamide, AMPS: 2-acrylamido-2-methylpropane sulfonic acid, GO: Graphene oxide

Table 2: Langmuir isotherm and Freundlich isotherm parameters for MB adsorption on AAm-AMPS, AAm-AMPS/Clay, and AAm-AMPS/GO.

Langmuir isotherm					
Sample	**Q_e (mg/g)**	**Q_{max} (mg/g)**	**R_L**	**K_L**	**R^2**
AAm-AMPS	11.54	18.15	0.4399	2.39	0.9804
AAm-AMPS/Clay	11.52	72.99	0.8608	0.21	0.9736
AAm-AMPS/GO	12.50	30.58	0.6502	1.05	0.9871
Langmuir isotherm					
Sample	**Q_e (mg/g)**	**K_F**	**n**	**1/n**	**R^2**
AAm-AMPS	11.54	4.69	1.49	0.67	0.9493
AAm-AMPS/Clay	11.52	10.21	0.91	1.01	0.9081
AAm-AMPS/GO	12.50	7.33	1.16	0.87	0.9183

MB: Methylene blue, AAm: Acrylamide, AMPS: 2-acrylamido-2-methylpropane sulfonic acid, GO: Graphene oxide

Table 3: Comparison of the various parameters of the present work with literature.

Pseudo-first-order kinetics						
No	**Polymer**		**Q_e mg/g**	**K_1**	**R^2**	**References**
1.	PAMPS	MB	8.83 13.64	0.002 0.001	0.543 0.556	[33]
2.	Kaolin clays (halloysite)	MB	10.11 18.54	0.015 0.005	0.78 0.65	[34]
3.	CMC/AAm hydrogel	MB	4.76 8.19	0.045 0.038	0.99 0.98	[35]
4.	Graphene oxide hydrogel	MB	13.29 19.65	0.01 0.007	0.252 0.140	[36]
5	AAm-AMPS	MB	11.39	0.012	0.91	Present work
6.	AAm-AMPS/Clay	MB	11.69	0.019	0.97	
7.	AAm-AMPS/GO	MB	13.79	0.011	0.98	
Pseudo-second-order kinetics						
No	**Polymer**	**Dye**	**Q_e mg/g**	**K_2**	**R^2**	**References**
1.	Kaolin clays (halloysite)	MB	8.09 13.21	0.003 0.001	0.38 0.40	[34]
2.	CMC/AAm hydrogel	MB	5.40 8.70	0.013	0.94	[35]
3.	Graphene oxide hydrogel	MB	14.32	0.022	0.841	[36]
4.	Graphene nanosheets	MB	15.14	0.0384	0.873	[37]
5	AAm-AMPS	MB	11.38	0.034	0.98	Present work
6.	AAm-AMPS/Clay	MB	11.69	0.036	0.99	
7.	AAm-AMPS/GO	MB	13.79	0.023	0.99	

AAm: Acrylamide, AMPS: 2-acrylamido-2-methylpropane sulfonic acid, GO: Graphene oxide, CMC: Carboxymethyl cellulose, PAMPS: Poly (2-acrylamido-2-methylpropane sulfonic acid)

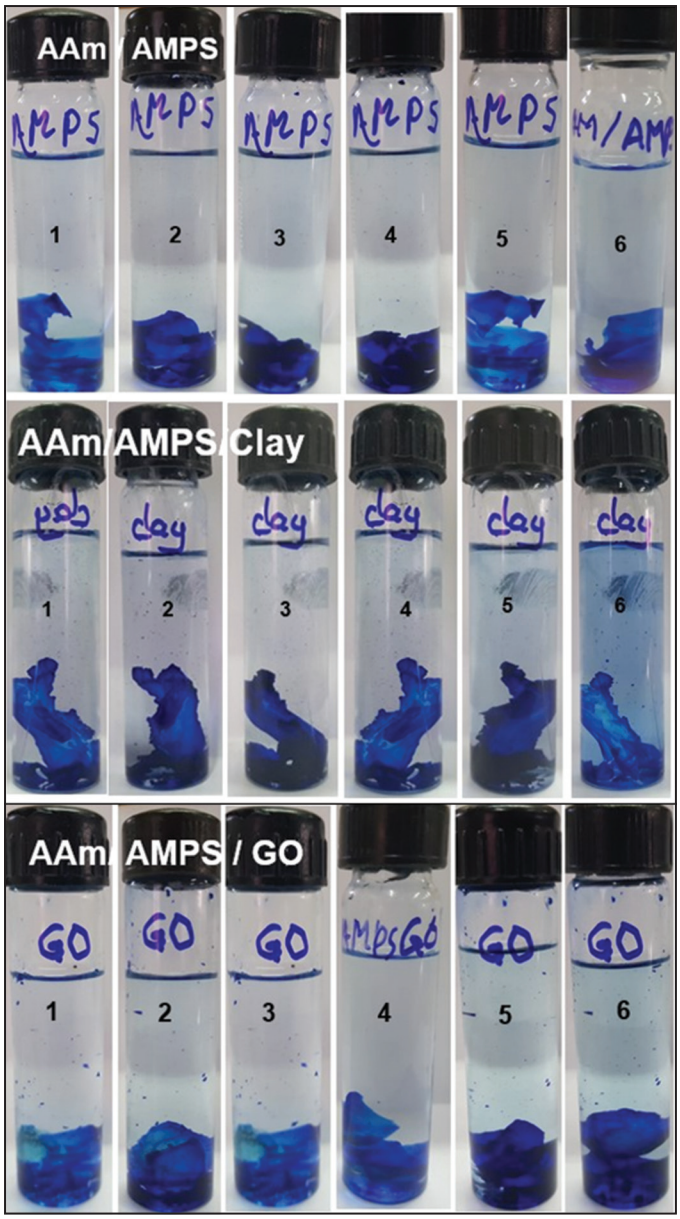

Figure 13: Reusability results for acrylamide-2-acrylamido-2-methylpropane sulfonic acid (AAm-AMPS), AAm-AMPS/Clay, and AAm-AMPS/Graphene oxide hydrogel for MB adsorption capacity.

4. CONCLUSION

AAm-AMPS hydrogel, AAm-AMPS/clay, and AAm-AMPS/GO nanocomposites hydrogels were prepared by in situ copolymerization in aqueous medium. It was found that the swelling degree of the hydrogel/GO nanocomposites was higher than that of the corresponding hydrogel at three different temperatures. The significant improvement of the swelling ratios of the hydrogel nanocomposites AAm-AMPS/GO might be mainly due to the plenty of functional groups on the GO sheets, such as -COOH, -C=O, -OH, and -C-O-C- that could

dramatically increase the density of the hydrophilic groups of the polymer networks. The adsorption of MB to AAm-AMPS hydrogel is a complex process involving several mechanisms, where heterogeneous and multilayer adsorption occurs as described by the Langmuir Isotherm and the Freundlich isotherm with a high adsorption capacity for MB dye. The hydrogel maintained good adsorption performance with more than >90% removal efficiency, which supports its use as a high-performance material in industrial remediation applications. MBA copolymer-based hydrogels of high adsorption capacities toward cationic contaminants dye (MB) are a new approach toward the hydrogel adsorbent for wastewater treatments.

5. ACKNOWLEDGMENTS

Authors Dr. K.S.V. Krishna Rao and Dr. Hlaing Hlaing Myint thank the Scholarship of ASEAN India Research and Training Fellowship (AIRTF) from the Department of Science and Technology (Government of India), Sanction of Federation of Indian Chambers of Commerce and Industry (FICCI) for financial support.

REFERENCES

1. S. Mondal, S. Das, A. K. Nandi, (2020) A review on recent advances in polymer and peptide hydrogels, ***Soft Matter***, **16(6):** 1404-1454.
2. K. S. V. Krishna Rao, C. S. Ha, (2009) pH sensitive hydrogels based on acryl amides and their swelling and diffusion characteristics with drug delivery behavior, ***Polymer Bulletin***, **62(2):** 167-181.
3. N. Sivagangi Reddy, S. Eswaramma, K. S. V. Krishna Rao, A. V. R. Reddy, J. Ramkumar, (2014) Development of hybrid hydrogel networks from poly(acrylamide-co-acrylamido glycolic acid)/ cloisite sodium for adsorption of methylene blue, ***Indian Journal of Advances in Chemical Science***, **2:** 107-110.
4. B. Sekizkardes, E. Su, O. Okay, (2023) Mechanically strong superabsorbent terpolymer hydrogels based on AMPS via hydrogen-bonding interactions, ***ACS Applied Polymer Materials***, **5(3):** 2043-2050.
5. A. K. Al-Shammari, E. Al-Bermany, (2022) Polymer functional group impact on the thermo-mechanical properties of polyacrylic acid, polyacrylic amide-poly (vinyl alcohol) nanocomposites reinforced by graphene oxide nanosheets, ***Journal of Polymer Research***, **29(8):** 351.
6. H. Khatooni, S. J. Peighambardoust, R. Foroutan, R. Mohammadi, B. Ramavandi, (2023) Adsorption of methylene blue using sodium carboxymethyl cellulose-g-poly (acrylamide-co-methacrylic acid)/Cloisite 30B nanocomposite hydrogel, ***Journal of Polymers and the Environment,*** **31(1):** 297-311.
7. Y. Huang, M. Zeng, J. Ren, J. Wang, L. Fan, Q. Xu, (2012) Preparation and swelling properties of graphene oxide/ poly(acrylic acid-co-acrylamide) super-absorbent hydrogel nanocomposites, ***Colloids and Surfaces A: Physicochemical and Engineering Aspects***, **401:** 97-106.
8. N. Sivagangi Reddy, K. Madhusudana Rao, T. J. Sudha Vani, K. S. V. Krishna Rao, Y. I. Lee, (2016) Pectin/poly(acrylamide-co-acrylamidoglycolic acid) pH sensitive semi-IPN hydrogels: Selective removal of Cu2+ and Ni2+, modeling, and kinetic studies, ***Desalination and Water Treatment***, **57(14):** 6503-6514.
9. T. J. S. Vani, N. Sivagangi Reddy, K. S. V. Krishna Rao, (2014) Adsorption studies of Eu3+ from aqueous solutions by poly(N'-isopropyl acrylamide-co-N-acryloyl-L-phenylalanine) hydrogel networks, ***Indian Journal of Advances in Chemical Science***, **2:** 111-114.
10. O. Akperov, E. O. Akperov, (2021) Removal of rhodamine 6G dye from water solution by alt-maleicanhydride-styrene copolymer, cross-linked with glycerine, ***Indian Journal of Advances in Chemical Science***, **9(3):** 166-173.
11. A. K. Anandrao, (2022) Removal of methylene blue by adsorption onto activated biomass of *Prunus cerasus*. Batch study, ***Indian Journal of Advances in Chemical Science***, **10(2):** 79-84.
12. A. E. Armand, K. Y. Urbain, Y. Y. Augustin, T. Albert, (2021) Adsorption of remazol black 5 and indigo carmine on corn cobs activated carbon: Kinetic, equilibrium, and thermodynamic studies, ***Indian Journal of Advances in Chemical Science***, **9(2):** 69-75.
13. M. G. Neumann, F. Gessner, C. C. Schmitt, R. Sartori, (2002) Influence of the layer charge and clay particle size on the interactions between the cationic dye methylene blue and clays in an aqueous suspension, ***Journal of Colloid and Interface Science,*** **255(2):** 254-259.
14. R. Kumar, R. K. Sharma, A. P. Singh, (2018) Removal of organic dyes and metal ions by crosslinked graft copolymers of cellulose obtained from the agricultural residue, ***Journal of Environmental Chemical Engineering***, **6(5):** 6037-6048.
15. N. Cao, Y. Zhang, (2015) Study of reduced graphene oxide preparation by Hummers' method and related characterization, ***Journal of Nanomaterials***, **2015(1):** 168125.
16. I. Clara, R. Lavanya, N. Natchimuthu, (2016) pH and temperature responsive hydrogels of poly(2-acrylamido-2-methyl-1-propanesulfonic acid-co-methacrylic acid): Synthesis and swelling characteristics, ***Journal of Macromolecular Science - Pure and Applied Chemistry***, **53:** 492-499.
17. E. Czarnecka, J. Nowaczyk, (2021) Synthesis and characterization superabsorbent polymers made of starch, acrylic acid, acrylamide, poly(vinyl alcohol), 2-hydroxyethyl methacrylate, 2-acrylamido-2-methylpropane sulfonic acid, ***International Journal of Molecular Sciences***, **22:** 4325.
18. K. Sahiro Y. Ide, T. Sano M. Sadakane, (2013) One-pot synthesis of microporous and mesoporous (NH4)3PW12O40 by reaction of *in-situ* generated PW12O403- with NH4+ in a strongly acidic solution, ***Materials Research Bulletin***, **48(10):** 4157-4162.
19. F. Ahmed Awadallah, S. Y. Abd El-Wahab, H. I. Al-Shafey, (2016) Controlled synthesis and characterization of nanohydrogels formed from copolymer (2-acrylamido-2-methylpropane sulfonic acid/acrylamide), ***E-Polymers,*** **16(3):** 207-215.
20. M. Rubinstein, R.H. Colby, A.V. Dobrynin, J.F. Joanny, (1996) Elastic modulus and equilibrium swelling of polyelectrolyte gels, ***Macromolecules***, **29:** 398-406.
21. F. Khoerunnisa, M. Nurhayati, R. N. Hiqmah, H. Hendrawan, F. Dara, H. A. Aziz, Y. Sonjaya, M. Nasir, (2021) 4th International Seminar on Chemistry. In: ***AIP Conference Proceedings***, Vol. 2349. p020025.
22. S. Lapwanit, T. Sooksimuang, T. Trakulsujaritchok, (2018) Adsorptive removal of cationic methylene blue dye by kappa-carrageenan/poly(glycidyl methacrylate) hydrogel beads: Preparation and characterization, ***Journal of Environmental Chemical Engineering,*** **6:** 6221-6230.
23. L. Li, L. Ferng, Y. Wei, C. Yang, H. F. Ji, (2012) Effects of acidity on the size of polyaniline-poly(sodium 4-styrenesulfonate) composite particles and the stability of corresponding colloids in water, ***Journal of Colloid and Interface Science***, **381:** 11-16.
24. Y. Zhou, J. Lu, Y. Zhou, Y. Liu, (2019) Recent advances for dyes removal using novel adsorbents: A review, ***Environmental Pollution***, **252:** 352-365.

25. M. T. Nakhjiri, G. B. Marandi, M. Kurdtabar, (2018) Poly(AA-co-VPA) hydrogel cross-linked with N-maleyl chitosan as dye adsorbent: Isotherms, kinetics and thermodynamic investigation, ***International Journal of Biological Macromolecules***, **117:** 152-166.
26. H. Mittal, A. Maity, S. S. Ray, (2015) Effective removal of cationic dyes from aqueous solution using gum ghatti-based biodegradable hydrogel, ***International Journal of Biological Macromolecules***, **79:** 8-20.
27. M. A. Al-Ghouti, D. A. Da'ana, (2020) Guidelines for the use and interpretation of adsorption isotherm models: A review, ***Journal of Hazardous Materials***, **393:** 122383.
28. I. Moreno-Villoslada, C. Torres, F. González, T. Shibue, H. Nishide, (2009) Binding of methylene blue to polyelectrolytes containing sulfonate groups, ***Macromolecular Chemistry and Physics***, **210:** 1167-1175.
29. V. Vimonses, S. Lei, B. Jin, C. W. K. Chow, C. Saint, (2009) Kinetic study and equilibrium isotherm analysis of Congo Red adsorption by clay materials, ***Chemical Engineering Journal***, **148(2-3):** 354-364.
30. S. S. Shah, B. Ramos, A. C. S. C. Teixeira, (2022) Adsorptive removal of methylene blue dye using biodegradable superabsorbent hydrogel polymer composite incorporated with activated charcoal, ***Water***, **14:** 3313.
31. I. Langmuir, (1918) The adsorption of gases on plane surfaces of glass, mica and platinum, ***Journal of the American Chemical Society***, **40(9):** 1361-1403.
32. K. Junlapong, P. Maijan, C. Chaibundit, S. Chantarak, (2020) Effective adsorption of methylene blue by biodegradable superabsorbent cassava starch-based hydrogel, ***International Journal of Biological Macromolecules***, **158:** 258-264.
33. A. M. Omer, W. A. A. Sadik, A. G. M. El-Demerdash, T. M. Tamer, R. E. Khalifa, M. S. Mohyeldin, N. A. Abdelwahed, (2021) Fabrication of semi-interpenetrated PVA/PAMPS hydrogel as a reusable adsorbent for cationic methylene blue dye: Isotherms, kinetics and thermodynamics studies, ***Polymer Bulletin***, **78(11):** 6649-6673.
34. A. Harrou, E. Gharibi, H. Nasri, M. El Ouahabi, (2020) Thermodynamics and kinetics of the removal of methylene blue from aqueous solution by raw kaolin, ***SN Applied Sciences***, **2(2):** 277.
35. N. F. Alharby, R. S. Almutairi, N. A. Mohamed, (2021) Adsorption behavior of methylene blue dye by novel crosslinked O-CM-Chitosan hydrogel in aqueous solution: Kinetics, isotherm and thermodynamics, ***Polymers***, **13(21):** 3659.
36. C. H. Chia, N. F. Razali, M. S. Sajab, S. Zakaria, N. M. Huang, H. N. Lim, (2013) Methylene blue adsorption on graphene oxide, ***Sains Malaysiana***, **42(6):** 819-826.
37. Ş. Parlayıcı, (2022) Natural mineral and biopolymers based adsorbent for cationic dyes removal: Glutaraldehyde crosslinked alginate/kaolin bead, ***Journal of Materials and Environmental Science***, **13(1):** 95-114.
38. F. Ali, N. Ali, I. Bibi, A. Said, S. Nawaz, Z. Ali, S. M. Salman, H. M. N. Iqbal, M. Bilal, (2020) Adsorption isotherm, kinetics and thermodynamic of acid blue and basic blue dyes onto activated charcoal, ***Case Studies in Chemical and Environmental Engineering***, **2:** 100040.
39. B. Salunkhe, T. P. Schuman, (2021) Super-adsorbent hydrogels for removal of methylene blue from aqueous solution: Dye adsorption isotherms, kinetics, and thermodynamic properties, ***Macromol***, **1(4):** 256-275.
40. H. Wang, L. Yi, F. Huang, Q. Huang, T. Zhou, (2024) Facile synthesis of graphene nanosheets on wastewater sediments for high efficient adsorption of methylene blue, ***Separation and Purification Technology***, **337:** 126366.